Biomass Conversion and Biorefinery (2023) 13:12179–12191
https://doi.org/10.1007/s13399-021-01962-4

ORIGINAL ARTICLE

Activated carbon derived from *Azolla filiculoides* fern: a high-adsorption-capacity adsorbent for residual ampicillin in pharmaceutical wastewater

Tariq J. Al-Musawi[1] · Nezamaddin Mengelizadeh[2] · Mahmoud Taghavi[3] · Samaneh Mohebi[4] · Davoud Balarak[5]

Received: 27 July 2021 / Revised: 9 September 2021 / Accepted: 13 September 2021 / Published online: 3 October 2021

Abstract
In this study, the effectiveness of activated carbon prepared from the *Azolla filiculoides* fern (ACAF) in order to remove ampicillin from aqueous solution was examined. The preparation of the ACAF was performed through chemical and physical activation processes with the presence of $ZnCl_2$ and at a temperature of 450 °C. The ACAF yield was 44.7% of the fresh *Azolla filiculoides*. The results obtained from the characterization study indicate that the prepared ACAF has excellent surface and internal properties to be used as an adsorbent. The surface area, porosity, and pore volume were estimated to be 716.4 m^2/g, 51.2%, and 0.621 cm^3/g, respectively. The functional groups in ACAF that were responsible for the adsorption of ampicillin molecules were detected using FTIR analyses. The maximum efficiency (96.84%) and uptake (114.3 mg/g) of ACAF to remove ampicillin were achieved under the following conditions: ACAF dose = 0.8 g/L, pH = 7, concentration of ampicillin = 100 mg/L, contact time = 60 min, and temperature = 45 °C. It was found that the kinetic and isotherm data matched the pseudo-second-order and Langmuir models with high precision values, respectively. Considering the thermodynamics of the adsorption, the endothermic and spontaneous nature of the ampicillin adsorption onto ACAF was approved. The ampicillin adsorption capacity by ACAF was not significantly affected by the presence of different concentrations of $NaNO_3$ competitor ion. The considerably higher adsorption capacity of the ACAF for ampicillin (114.3 mg/g) than other previously used adsorbents with excellent regeneration level (five cycles) depicts the superior performance of ACAF in the adsorption systems.

Keywords Adsorption · Ampicillin · Activated carbon · Characterization · Isotherm · Kinetic

1 Introduction

Over the past decades, there has been great interest emanating from many studies on the increasing prevalence of various pollutants in rivers, lakes, groundwater, and soil originating from a large variety of activities including chemical and petrochemical industries, pharmaceutical and veterinary industries, in addition to personal care products. In addition, the recent COVID-19 pandemic caused an increase in the global production of medicines for the purpose of addressing the health consequences of this disease including for products to diagnose, mitigate, or prevent COVID-19, and for other critically needed products to treat symptoms of COVID-19 or to provide supportive care to those with COVID-19. This, in turn, will certainly lead to the entry of some of different compounds into the aquatic environment, which is associated with risks for human health and pollution of ecosystems. Among many pharmaceutical

✉ Davoud Balarak
dbalarak2@gmail.com

[1] Department of Chemical Engineering and Petroleum Industries, Al-Mustaqbal University College, Babylon, Iraq

[2] Department of Environmental Health Engineering, Evas Faculty of Health, Larestan University of Medical Sciences, Larestan, Iran

[3] Department of Environmental Health Engineering, Social Determinants of Health Research Center, Gonabad University of Medical Sciences, Gonabad, Iran

[4] Student Research Committee, Zahedan University of Medical Sciences, Zahedan, Iran

[5] Department of Environmental Health, Health Promotion Research Center, Zahedan University of Medical Sciences, Zahedan, Iran

pollutants in the environment, antibiotics are widely used in the fields of combating and in the treatment of human and veterinary bacterial diseases [1, 2]. For instance, one of the extensively employed antibiotics is ampicillin. Ampicillin is one of the β-lactam antibiotics [3]; it is used to treat a wide range of bacterial infections affecting humans and livestock, such as bladder, ear, respiratory, reproductive system, and gastrointestinal tract infections [4–6]. Through binding to peptidoglycan-synthesizing enzymes, ampicillin hinders the synthesis of the cell wall of bacteria.

In fact, the environmental contamination by antibiotics can lead to serious consequences for human health and aquatic biota depending upon the pollutant's concentration and exposure time. Although the contamination from antibiotics is limited (normally in concentrations below the µg/L level), their risks lie in long-term exposure via drinking water or food to these compounds. Moreover, one of the important issues which has been identified for presence of this kind of pollutants in the environment is the development of the phenomenon of antibiotic-resistant bacterial diseases [7]. In addition, these compounds have the possibility of producing highly toxic or carcinogenic byproducts during the course of their degradation in the environment, or their interaction with other natural or anthropogenic pollutants [8–10]. The most important example of this is the interaction of pharmaceutical compounds with chlorine, or ozone added for disinfection purposes in drinking-water plants [11]. Therefore, there is an urgent need to address and mitigate the negative effects of the environmental pollution with antibiotics by applying an efficient method of treatment of wastewater containing antibiotics [12–14]. The focus is currently on devising simple, cost-effective, and efficient methods that ensure reducing these pollutants to the internationally permissible limits [13, 15, 16].

Recently, different techniques have been applied in pharmaceutical compounds for the purpose of removal of aqueous solutions including flocculation, flotation, photocatalysis, membranes, adsorption, and oxidation techniques [17, 18]. Among the multitude of treatments, the adsorption method has attracted substantial attention by several environmental researchers in the treatment of wastewater containing hazardous pollutants. Adsorption is universal and is the preferential treatment process for removing different types of elements because of its high efficiency, simplicity in design and operation, high-quality effluents, cost-effectiveness, and feasibility [19, 20]. Major mechanisms responsible for the removal of pollutants by the adsorption include chemical reactions, bonding processes, electrostatic processes, and ion exchange. From another side, the adsorption process is a sensitive process and its applicability and efficiency in the removal are highly dependent on the nature of the adsorbent used. Many adsorbents, such as commercial activated carbon (CAC), have been found to possess a high capacity for removing diverse types of pollutants from liquid wastes [21–23]. However, CAC is not a cheap adsorbent especially when it was used in a large-scale treatment process, and the regeneration process of this adsorbent is complex [24–26]. The best technique to overcome these disadvantages is the derivation of activated carbon (AC) from a low-cost plant or agricultural wastes, which is the main objective of this study, and which has been reported as a good alternative compared to expensive CACs [27]. Hence, algae, ferns, and other natural plants are one of the best carbon sources, and they are actually one of the cheapest raw materials as well. Among the natural plants, *Azolla filiculoides* (AF), which is a floating water fern, has evoked a great interest in the water treatment using the adsorption technique [28, 29]. This fern is grown in bulk in several locations in the world, like in the north of Iran, and is usually consumed as fodder by livestock, or used as fertilizer [30, 31].

The purpose of this work was to prepare AC from AF (named ACAF) and examine its adsorption capacity to remove ampicillin from polluted solutions. The chemical properties, surface, and structural properties were determined using powerful characterization techniques. In addition, the adsorption performance of ACAF for the removal of ampicillin was examined at different values of environmental parameters. The isotherm, kinetic, and thermodynamic capacities of ampicillin adsorption onto ACAF were also discussed. Ultimately, the regeneration potential of the ACAF was tested through five adsorption–desorption cycles.

2 Materials and methods

2.1 Chemicals

Ampicillin (chemical formula: $C_{16}H_{19}N_3O_4S$, molecular mass: 349.4 g/mole) was purchased from Sigma-Aldrich Co., USA. The stock solution of ampicillin (1000 mg/L) and other working solutions were prepared via dilution using double-distilled water. The other reagents/chemicals used in the current work were of analytical grade.

2.2 Adsorbent preparation

The ACAF was prepared from AF using both chemical and physical activation techniques. The chemical activation was accomplished by using $ZnCl_2$ as a dehydration agent, whereas the physical activation was carried out by a heating process at high temperature. First, the required quantity of AF was obtained from an open area in Anzali wetland (Iran). Note that the unit cost of collecting 1 kg of fresh AF was < US$ 1. Next, the collected AF was dried, crushed to a powder, and finally sieved to uniform particles (0.45 mm). Subsequently, the AF powder was soaked in a $ZnCl_2$ solution

(28%) for 12 h. After that, this mixture was placed in a stainless steel reactor (placed in a temperature-controlled vertical furnace) under a high-purity N_2 atmosphere at a flow rate of 300 cm^3/min. The mixture was gradually heated to a temperature of 450 °C and kept at this temperature for 1 h. At this stage, the resultant solid particles were ACAF, which was subsequently subjected to acid treatment using hot HCl (0.5 M) in order to remove excess $ZnCl_2$. The ACAF was separated from solution via filtration, washed with warm water, dried in a digital oven at 105 °C for 24 h. The percentage yield of synthesized ACAF can be determined using Eq. 1 [32].

$$Yield = \frac{W_C}{W} \times 100 \quad (1)$$

where W_C and W are the weights of obtained ACAF and dried AF, respectively.

2.3 Characterization of ACAF

The changes in the topographical characterization of the ACAF before and after ampicillin adsorption process were observed by FESEM images, which were taken using high-resolution scanning electron microscopy (S-4800F, HITACHI). N_2 adsorption–desorption technique (at a temperature of = − 196 °C) using a Micromeritics-TRISTAR-3000 surface area and porosity analyzer was utilized for exploration of the surface area, porosity, and total pore volume of ACAF. The elemental analysis was conducted by using Perkin Elmer elemental analyzer (Model EA2400II). FTIR was performed using a model device Thermo Nicollet AVATAR 5700 using the KBr pellet method in the range 400–4000 cm^{-1}. The experimental steps of analysis of point of zero charge (pH_{pzc}) are shown in the supplementary information file (Section S1).

2.4 Experiments and calculations

The adsorption experiments were conducted in a series of 200-mL Erlenmeyer flasks filled with 100 mL of ampicillin solution of predetermined concentration. The adsorbents added in each flask were stirred with an ampicillin solution at stirring speed of 150 rpm. The ACAF adsorption capacity for ampicillin was determined at different conditions: pH (3–11) which is regulated through dropwise addition of NaOH and/or HCl solution (0.1 M), initial ampicillin concentration (25–100 mg/L), adsorption time (0–120 min), ACAF dose (0.1–0.5 g/L), temperature (15–45 °C), and concentration of competitor $NaNO_3$ ion (0–0.5 mol/L). The regeneration experiment of spent ACAF was performed in five consecutive adsorption–desorption cycles of ampicillin under the following experimental conditions: ACAF dose = 0.8 g/L, pH = 7, initial ampicillin concentration = 25 mg/L, adsorption time = 60 min, and temperature = 25 °C.

At a specific time of adsorption reaction, a 3-mL sample was taken from each solution and quickly centrifuged at 1509 × g for 10 min. Determination of the initial and remaining ampicillin concentration in solutions was done using HPLC (Kenaver HPLC device) with C18 column, and detection was measured at $\lambda = 215$ nm with a diode array UV–Vis detector after centrifugation of solution sample (10 mL) at 3600 rpm for 10 min. The dihydrogen phosphate (pH = 3.5)-acetonitrile (87.5:12.5, v/v) was the mobile phase employed, which delivered at a flow rate of 1.00 mL/min. The removal efficiency (% removed) and adsorption capacity (q_t) of ampicillin molecules onto ACAF were determined using Equations (S1) and (S2) shown in the supplementary information file (Section S2). For the kinetic and thermodynamic studies, the results of the experiments of the ACAF adsorption capacity at different ampicillin initial concentrations and temperatures were used, respectively. In addition, an experiment was performed to determine the relationship between the ACAF adsorption capacities toward ampicillin at a different temperature (15–45 °C), and the results of this experiment were used for the isotherm study. In addition, for selecting the best models, the determination correlation coefficient (R^2) and normalized standard deviations Δq (%) (Equation S3: supplementary information file) values were employed in the isotherm and kinetic studies.

3 Results and discussion

3.1 Characterization analyses

It was found that the main elements that formed ACAF are carbon (51.2%), hydrogen (4.18%), nitrogen (0.73%), and oxygen (40.71%). The ash content in the ACAF sample was 2.84%. Using Eq. 1, the percentage yield of synthesized ACAF adsorbent from AF fern was found to be 44.7% at the cost of US$ 10/kg. Table 1 lists the results of the specific surface area, pore size, and other characteristics of ACAF.

Figure 1 illustrates the FESEM images of the ACAF before and after ampicillin adsorption. From the FESEM image before adsorption, the ACAF can be described as having many pores as well as having many fragments scattered on its surface and inside the pores. In fact, these properties,

Table 1 Surface and pore characteristics of ACAF

Specific surface area	Average pore diameter	Pore volume	Porosity	Bulk density	Moisture content
716.4 m^2/g	41.3 nm	0.621 cm^3/g	51.2%	0.693 g/cm^3	2.21%

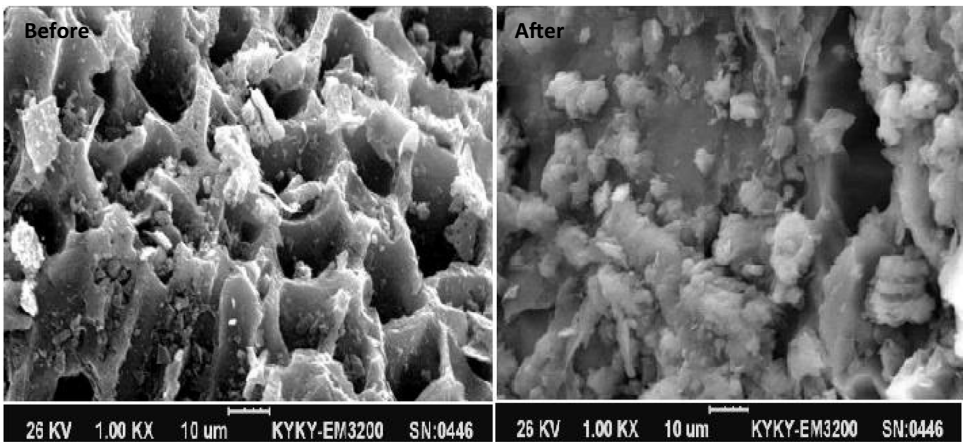

Fig. 1 SEM images of ACAF before and after ampicillin adsorption

which are highly favorable in the adsorption process, are characterized by many carbon adsorbents synthesized from agricultural materials, and this results from exposure of these materials to high temperatures during the synthesizing process [33]. After ampicillin adsorption, it can be seen that the surface characterization of used adsorbent was completely changed. All the previous detected pores disappeared and the surface became more flat. In addition, the fragments became larger. These changes can be reasoned to have occurred from the attachment and sorption of ampicillin molecules on the surface and pores of ACAF.

The N_2 adsorption–desorption and pore size distribution analyses of ACAF are presented in Fig. 2. This figure was indicative of A type IV isotherm by the hysteresis loop at high P/P_0 values. Moreover, the pore diameter range of 4–5 nm was determined for ACAF particles.

Nomination of bonds in the synthesized ACAF adsorbent (before and after ampicillin adsorption) was done using FTIR analysis (in the range of 400–4000 cm^{-1}) (Fig. 3). In this figure, shifting and disappearance of some peaks and the appearance of some new peaks could be noticeable, which was representative of this fact that, in the adsorption of ampicillin, the functional groups on the surface of the ACAF are affective. Table 2 lists the details of the FTIR analysis employed for our studied adsorbent. From this table, it can be seen that it was the functional

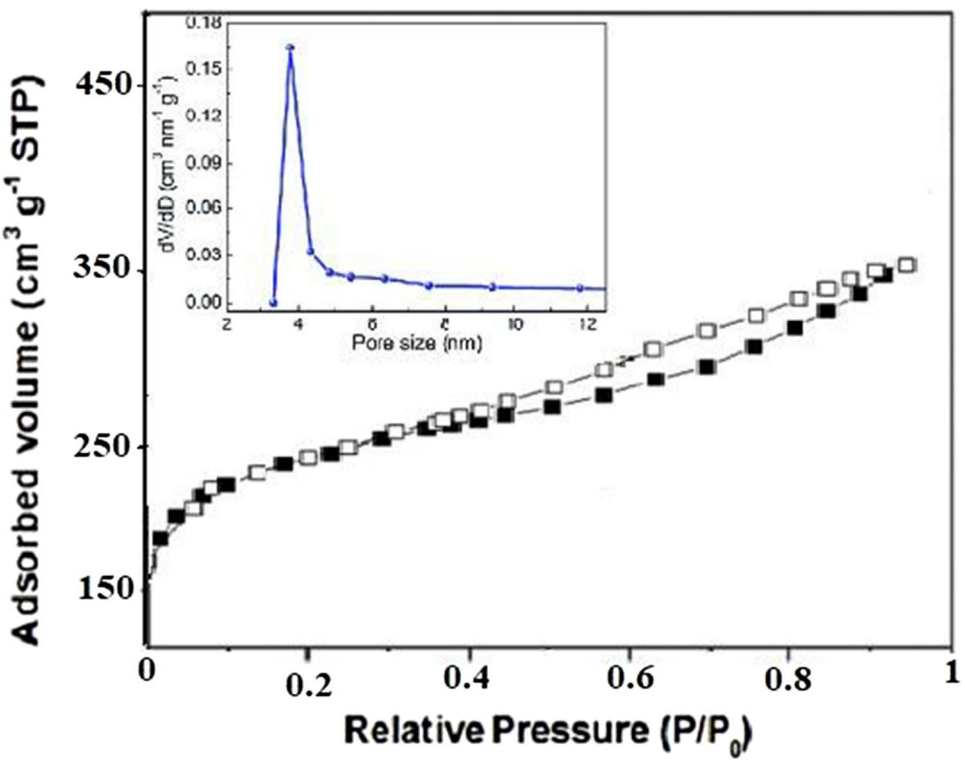

Fig. 2 N_2 adsorption–desorption isotherms and BJH pore size distribution curves

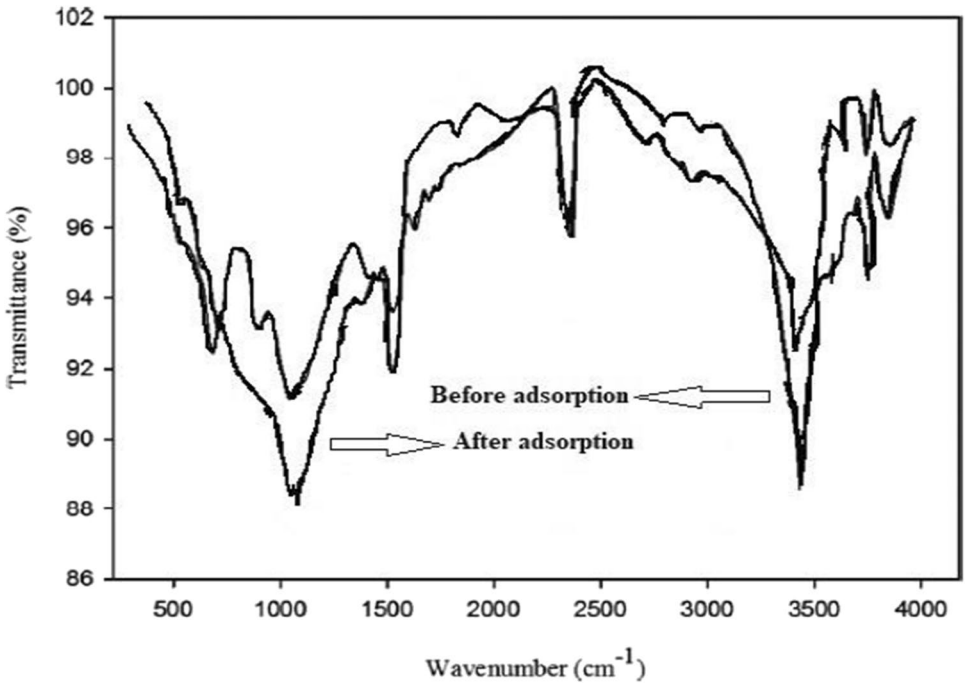

Fig. 3 FTIR spectra of ACAF samples (temperature = 150 °C)

Table 2 Functional groups that were detected in the FTIR spectra of ACAF samples before and after ampicillin adsorption

Assignment	Detected peaks after adsorption (cm^{-1})	Detected peaks before adsorption (cm^{-1})
–C–H bending and C–Cl stretch (strong)	Not detected	725
–C–H out-of-plane bending	Not detected	921
–C–O stretch (strong)	1053	1045
–N–O stretch (strong)	1378	Not detected
–N–O stretch (strong, two bonds) nitro	1526	1525
C = O stretch and stretch (strong)	Not detected	1742
–C≡C stretching	2355	2355
–CH stretch (strong)	2924	2924
–OH stretch, H-bonded	3445	3466
$–NH_2$ stretching	3788	3778

groups which were responsible for adsorption of the ampicillin molecules.

3.2 Effect of ACAF dosage

By varying the ACAF dosage in the aqueous solution (0.1–1.5 g/L), the evaluation of effect of ACAF dose on the adsorption efficiency of ampicillin was reckoned (Fig. 4). As elucidated by this figure, an improvement in ampicillin removal from aqueous was detected as the ACAF mass was increased; however, for dose of ACAF > 0.8 g/L, no change in efficiency values was observed. Accordingly, an enhancement in ampicillin adsorption efficiency from 39.26 to 96.84% was noticed due to an increase in dosage from 0.1 to 0.8 g/L; this results in the improvement in the number of active sites for adsorption [34]. Moreover, as illustrated in Fig. 4, the q_e can be affected by effect of ACAF mass; so that an increase in ACAF mass (0.1 to 1.5 g/L) leads to diminish it (98.15 to 16.26 mg/g). This may be explained according to the collision of adsorbent particles with each other and the formation of bulk; this reduces the active sites for adsorption of ampicillin [35].

3.3 Effect of pH and mechanism of adsorption

The variation of pH values has been detected to be associated with a remarkable effect on the adsorbent surface and ampicillin ionization in solution [36]. The results of studying this parameter are shown in Fig. 5. The values of pK_1 (–COOH) and pK_2 ($–NH_3^+$) of ampicillin have been detected

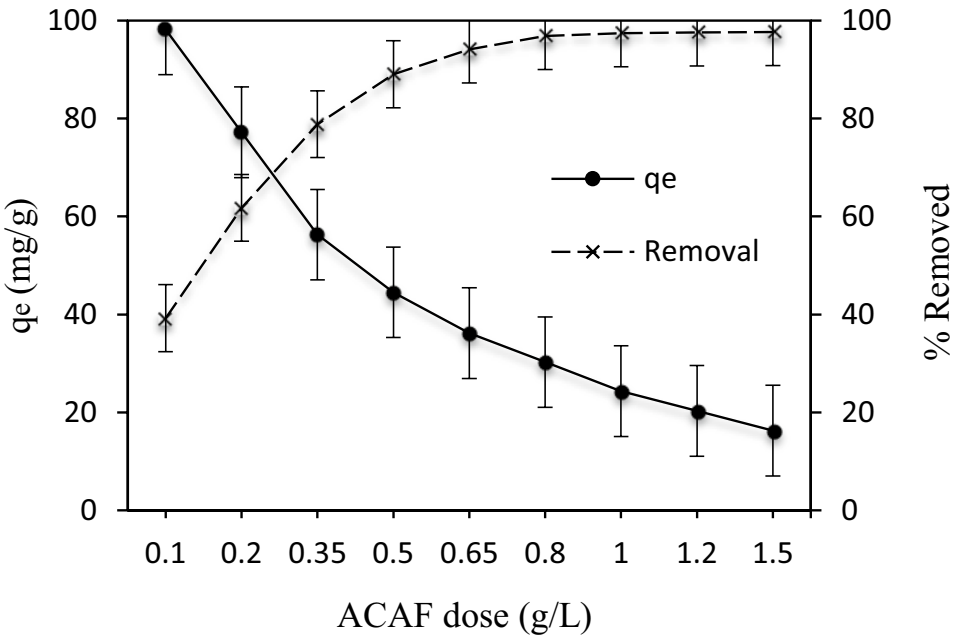

Fig. 4 Effect of ACAF dosage on efficiency of ampicillin adsorption (C_0: 25 mg/L, temperature = 30 ± 2 ℃, pH: 7, time: 60 min)

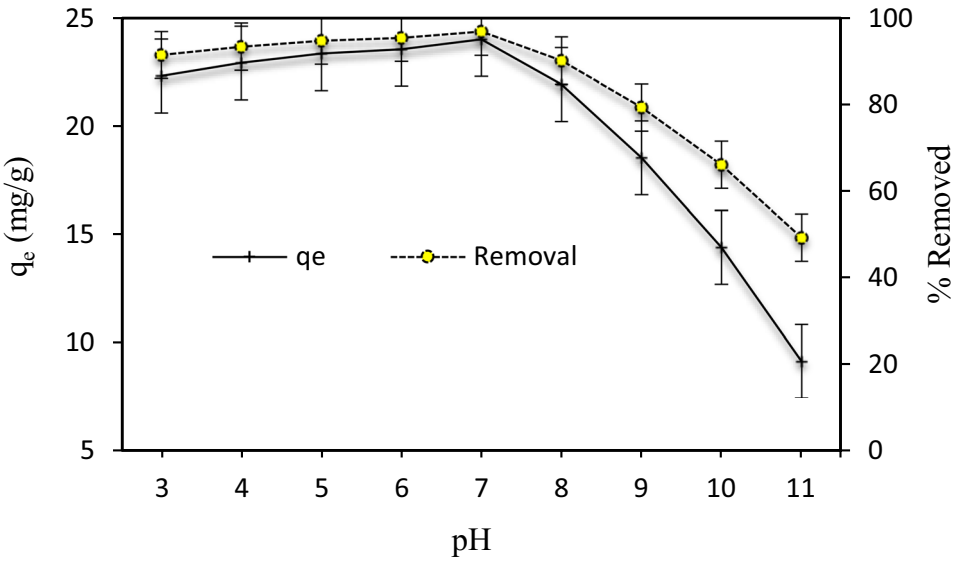

Fig. 5 Effect of pH on the ampicillin adsorption onto ACAF (C_0: 100 mg/L, temperature = 30 ± 2 ℃, time: 60 min, ACAF dosage: 0.8 g/L)

to be 2.5 and 7.3, respectively. Thus, deprotonation of protonated ampicillin containing –COOH and $–NH_3^+$occurs in the pH ranges 2–4 and 6–8, respectively [37]. According to the results, removal percentage was developed with an increase in pH values from 3 to 7; however, after that, a gradual decrease in the removal efficiency up to a pH of 11 was detected. Moreover, at a pH of 7, the highest removal percentage of 96.84% was detected. Describing this event is done based on this fact that both ACAF and ampicillin have positive charges at pH < 2.5; this diminishes the adsorption of ampicillin onto ACAF surface [38]. However, deprotonation of ampicillin occurs at a pH of 7. This leads to formation of negative sites to interact with the positive surface of ACAF, which provides the highest adsorption of ampicillin in the mentioned pH value (pH = 7). In addition, the adsorption of ampicillin was declined at pH values higher than 7. The formation of electrostatic repulsion forces between carboxylate groups present in ampicillin molecules and the negative surface charges of the ACAF could describe the observed event in these pH values [39]. Moreover, it is expected that π-π interaction between a benzene ring of ampicillin and ACAF happens, which leads to the developing of adsorption capacity [40].

As shown in Figure S1, the point of zero charge (pH_{zpc}), which can be useful for justifying adsorption at a low pH, was 7.6. ACAF in the solution pH lower than the mentioned

value, that is, 7.6, have positive charges, while for the solution with a pH higher than 7.6, the adsorbent had negative charges [41]. Therefore, the presence of a negative charge in the surface of ACAF at pH values higher than 7.6 leads to a decline in the removal efficiency due to electrostatic repulsion between negatively charged ampicillin species and the negatively charged ACAF. Another reason for this event is the existence of a higher concentration of OH^- ions in the working solutions [42].

3.4 Effects of initial ampicillin concentration and kinetic study

The examination of the changes in ampicillin removal efficiency by varying the initial ampicillin concentration was done using 100 mL solution of initial concentrations of 25, 50, 100, and 200 mg/L and 0.8 mg of ACAF, and the results of this part are reported in Fig. 6. In this figure, rapid ampicillin adsorption is detected in the beginning and after that, some minor enhancement is observed until it reaches equilibrium. Since the active site on ACAF surface is more accessible in the start of process, adsorption of ampicillin speedily occurs at the initial contact time. As mentioned, there is a slow rate of adsorption after this stage. A description of this reason can be done based on the slow pore diffusion of the adsorbate molecule into the bulk of the adsorbent [43, 44]. Since the maximum adsorption rate was obtained at 60 min and the process reached equilibrium at this contact time, 60 min was considered equilibrium contact time for the next experiments. In addition, q_e (adsorption capacity at equilibrium) was observed to be developed from 30.35 to 189.25 mg/g by increasing the initial ampicillin concentrations (from 25 to 200 mg/L). By increasing the initial concentration of adsorbate, the driving force of the concentration gradient is developed, which may be the reason for the enhancement of q_e [45].

Analyzing the kinetic data (Fig. 6) was done by pseudo-first-order (PFO) (Equation S4) and pseudo-second-order (PSO) (Equation S5) models [46, 47]. More information about the theoretical background used in this study is presented in the supplementary material file (Section S2). The kinetic parameters (e.g., correlation coefficients, R^2, and normalized standard deviations, Δq (%)), which are determined using the linearized kinetic plots of PFO and PSO (Fig. 7), are documented in Table 3. Through calculating R^2, and Δq (%), and the agreement between the calculated q_e cal and the experimental q_e exp values, the best kinetic model for describing the obtained data is determined. As determined, for PSO, higher R^2 values were obtained compared to the PFO model. In addition, the values of Δq (%) for PSO were found to be much lower compared to the values for PFO model. In addition, it was found that the closeness of values of the q_e cal and the q_e exp for PSO model was greater than the PFO model. The above results are indicative of more appropriateness of the PSO model for enlightening the behavior of the studied process. Furthermore, increasing the initial ampicillin concentration and surface loading has led to a decrease in the values of K_2. With an increase in initial concentration of studied pollutant and surface loadings, diffusion efficiency is declined and the competition of ampicillin molecules for fixed reaction sites is raised. This results in lower K_2 values.

Owing to the inability of the kinetic models mentioned above for defining a diffusion mechanism, the kinetic data were fitted by intra-particle diffusion model (IPD) model (Equation Section S5: supplementary material). When the

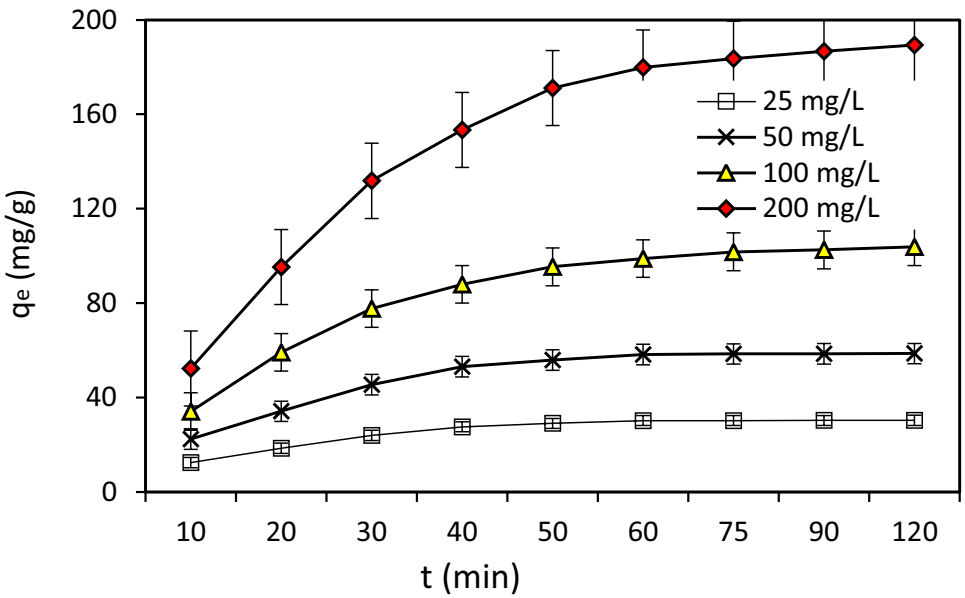

Fig. 6 Effect of contact time on the adsorption capacity of ampicillin (pH = 7, ACAF dosage 0.8 g/L, and temperature = 30 ± 2 ℃)

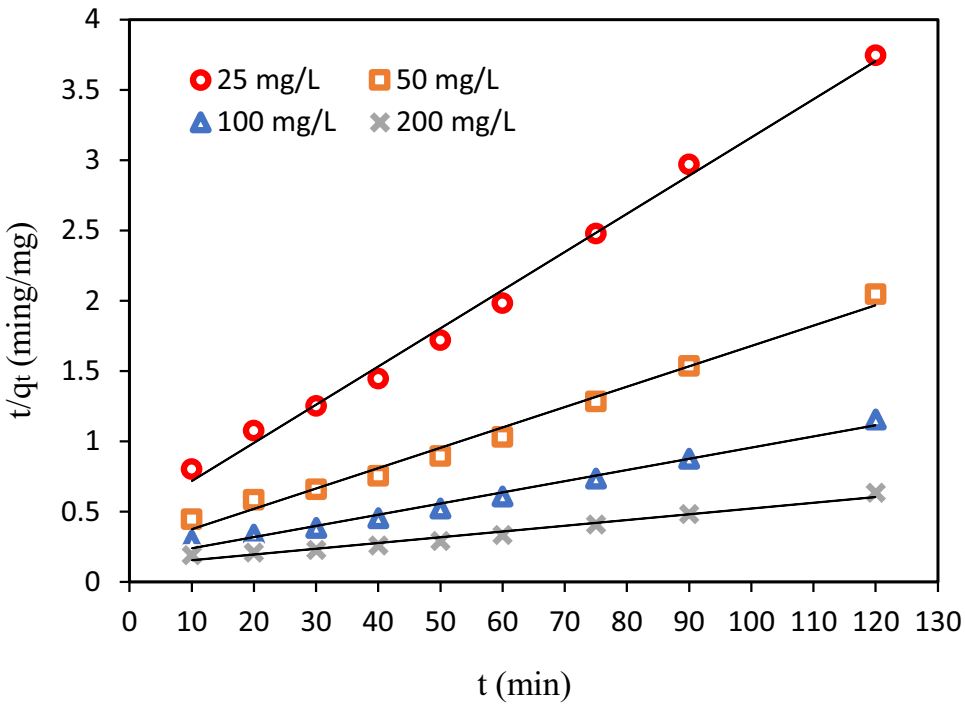

Fig. 7 Pseudo-second-order kinetic plots for adsorption of ampicillin on ACAF

Table 3 The results of kinetic model studies related to the ampicillin adsorption onto ACAF

Concentration (mg/L)	$(q_e)_{exp}$	Intra-particle diffusion			Pseudo-first order				Pseudo-second order			
		K	I	R^2	$(q_e)_{cal}$	Δq (%)	K_1	R^2	$(q_e)_{cal}$	Δq (%)	K_2	R^2
25	30.35	3.95	1.96	0.837	14.89	3.24	0.09	0.921	36.93	0.582	0.0016	0.993
50	58.65	7.14	2.34	0.815	36.54	1.77	0.08	0.908	68.22	0.338	0.0009	0.996
100	103.2	8.46	3.76	0.772	58.64	2.33	0.05	0.885	116.1	0.195	0.0003	0.997
200	189.3	11.72	5.14	0.767	123.9	4.49	0.04	0.896	213.9	0.211	0.0001	0.995

mechanism of adsorption process obeys the IPD, drawing the q_t vs. $t^{1/2}$ provides a straight line; the slope and intercept of the plot are used for the K and I, respectively. As can be seen in Fig. 8, IPD plots were not linear over time. This highlights the existence of more than one mechanism affecting the ampicillin adsorption for ACA. Furthermore, the plots do not pass through the origin. According to the foregoing, the presence of IPD is confirmed, but in addition to this, there are other mechanisms that act as rate-controlling steps. In Table 3, values obtained for K and I have been reported, According to this table, an increase in initial concentration is associated with enhancing K values, which is explained by an increase in the driving force that occurs due to initial concentration and adsorption through mesopores and micropores [47]. In addition, I values were observed to be greater than 0, and increasing the initial ampicillin concentration has led to the enhancement of its values. Considering this fact, boundary layer diffusion might be the rate-limiting step in the adsorption process, not intra-particle diffusion [48].

3.5 Equilibrium isotherms

In this study, the equilibrium data was modeled with four isotherm models, including Freundlich, Langmuir, Dubinin-Radushkevitch, and Temkin (Section Section S3: supplementary information). The results of each model's parameters are listed in Table 4. It can be seen that the determined range of R_L value was 0.043 to 0.177 at temperatures of 15–45 °C. This is demonstrative of the favorable adsorption of ampicillin onto ACAF. In addition, a diminution in R_L values was detected when the temperature increased from 15 to 45 °C. This reveals that higher temperatures are significantly favorable for the adsorption of ampicillin. According to the results, the highest ampicillin adsorption capacities onto ACAF at different temperatures were 89.92, 96.74, 105.2, and 114.3 mg/g, respectively. These values were comparable to values obtained for some other adsorbents. The details are provided in Table 4.

According to the values of n, the adsorption process is linear when $n = 1$, the chemical adsorption occurs when

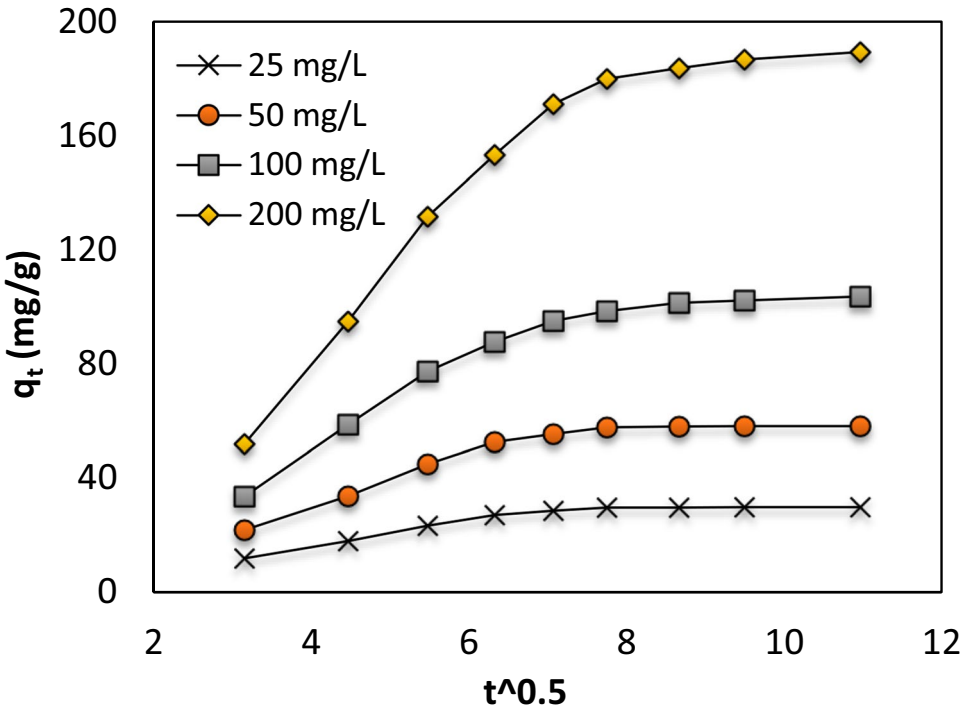

Fig. 8 Intra-particle diffusion kinetic plots for adsorption of ampicillin on ACAF

Table 4 Isotherm parameters for adsorption of ampicillin onto ACAF at various temperatures

Models	15 °C	25 °C	35 °C	45 °C
Langmuir				
q_m (mg/g)	89.92	96.74	105.2	114.3
K_L (L/mg)	0.0462	0.0638	0.106	0.219
R_L	0.177	0.135	0.086	0.0435
R^2	0.994	0.996	0.997	0.998
Freundlich				
K_F	17.13	26.19	33.71	51.35
$1/n$	0.925	0.675	0.443	0.236
R^2	0.917	0.891	0.866	0.783
Temkin				
K_T	14.32	18.39	30.8	50.1
b	31.91	37.33	50.11	69.70
R^2	0.981	0.962	0.941	0.866
D-R				
q_m (mg/g)	38.99	52.57	66.12	83.56
E	3.54	4.92	6.11	7.35
R^2	0.749	0.634	0.677	0.721

$n < 1$, and the adsorption is a physical process when $n > 1$ [49]. The intercept and slope of the plot of $\ln q_e$ against $\ln C_e$ (not shown) are employed for determining constants of K_F and n. In this study, according to the results of the Freundlich isotherm, the values of n were observed to be less than 1 for all studied temperatures. This specifies the physisorption nature of the process. In addition, an increase in values of the Freundlich constant (K_F) at higher temperatures is representative of the favorability of higher temperatures for the adsorption process. Furthermore, since, in the present study, the $1/n$ value observed at temperatures studied was lower than unity, and adsorption of ampicillin onto ACAF was favorable.

The calculation of constants of K and q_m of D-R model is done through employing the slope and intercept of the plot, which was obtained from drawing $\ln q_e$ against ε^2 (not shown). E values obtained were 3.54, 4.92, 6.11, and 7.35 kJ/mol, at 15, 25, 35, and 45 °C, respectively. The mentioned values were observed to be less than 8 kJ/mol under studied experimental conditions (Table 2); this highlights the physisorption nature for adsorption of ampicillin onto ACAF.

Calculating b and K_T of the Temkin model is done based on the slope and intercept of the line which is obtained by drawing q_e against $\ln C_e$ (not shown). This is representative of improving the heat of adsorption of ampicillin onto the surface of ACAF when temperature (from 15 to 45 °C) increases. It also agrees with the endothermic and thermodynamic results found for sorption. Moreover, since values of b were observed to be lower than 80 kJ/mol, a physical adsorption process occurred. Comparison of correlation coefficient (R^2) achieved for studied isotherm models (Table 4), aptness of the Langmuir model for portraying the adsorptive behavior was confirmed since R^2 of this model was greater than the other studied models. Moreover, on the

Table 5 Comparison of adsorption capacities of various adsorbents for ampicillin

Adsorbent	Uptake	Reference
Granular activated carbon	12.70	[3]
Montmorillonite	27.60	[4]
Natural bentonite	50.35	[36]
Organo bentonite	86.55	[36]
Activated carbon-graphene slurry	1.87	[39]
Polydopamine/zirconium (IV) iodate	100	[38]
Hydroxyapatite-C/Fe_3O_4	3.49	[40]
Porous hydroxyapatite	47.20	[37]
Dense hydroxyapatite	39.70	[37]
Mesoporous silica: SBA-15	44.10	[5]
Mesoporous silica: MCM-41	39.70	[5]
Boron nitride nanocone	24.10	[6]
ACAF	114.30	This study

basis of the results of the best fit model, homogenous surface of the ACAF was predicted for the adsorption of ampicillin molecules from aqueous solution.

In Table 5, the highest adsorption capacity of ACAF for adsorption of ampicillin has been compared with the others. According to the results of this comparison, the adsorption capacity of ACAF is high compared to most of the reported adsorbents, which indicates the suitability of this adsorbent for use in the adsorption processes.

3.6 Adsorption thermodynamics

Considering the results related to this part of the study, the values for ΔG^o were observed to be negative; so that − 2.94, − 3.84, − 5.73, and − 8.69 kJ/mol were calculated at 15, 25, 35, and 45 °C, respectively. On the basis of those negative values, the adsorption process was considered to be spontaneous [50, 51]; nevertheless, increasing the temperature has provided the enhancement in absolute values of ΔG^o. It indicates that the adsorption is more feasible when the temperature is high. Moreover, according to values of ΔG^o (within the ranges of − 20 and 0 kJ/mol), the adsorption mechanism was identified to be mainly physical [52]. In addition, the value of ΔH^o obtained was 19.82 kJ/mol, which was a positive value. Positive values for this parameter are demonstrative of an endothermic nature for adsorption processes. In addition to clarification of the above-mentioned nature, the type of adsorption (either physical or chemical) can be detected based on the magnitude of ΔH^o [53]. The values obtained for ΔH^o (from 2.1 to 20.9 kJ/mol) highlight that fact that studied adsorption process is of the physisorption type. The positive value obtained for ΔS^o (0.188 kJ/mol. K) represents the presence of the attraction of ACAF for ampicillin. It is also indicative of enhancing randomness at the solid-solution interface in the adsorption process [54].

3.7 Effect of ionic strength

Evaluating the effect of ionic strength on the adsorption of ampicillin was done through conducting experiments with $NaNO_3$ (the electrolyte in the range of 0 to 0.5 mol/L). The possible competition which may occur between Na^+ and NO_3^- ions and ampicillin adsorption for adsorption sites or formation of general effect of bionic atmosphere or saline effect can affect the adsorption of the pollutant onto studied adsorbent. Nevertheless, our observation provided in Fig. 9 is indicative of the immaterial effect of ionic strength on

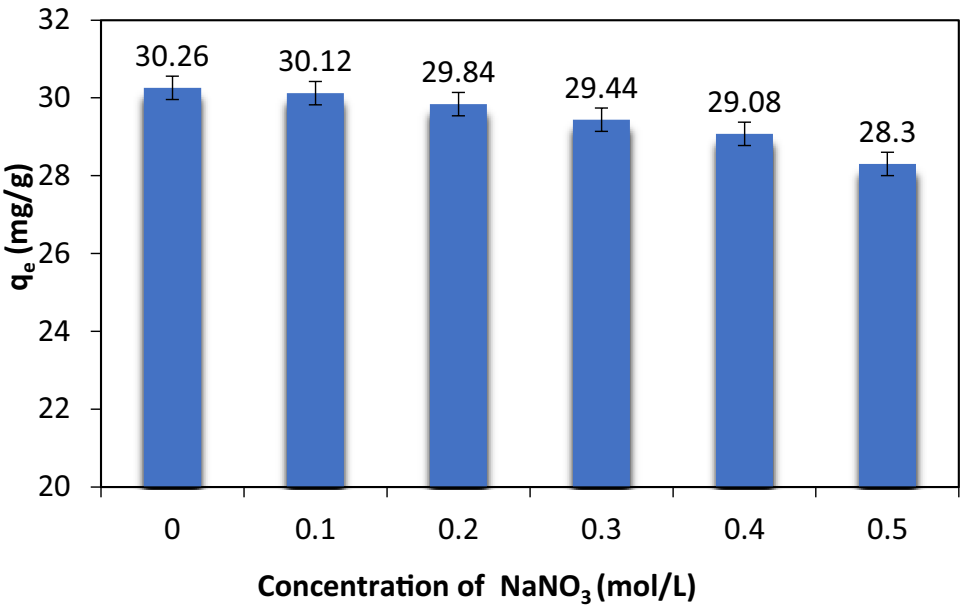

Fig. 9 Effect of ionic strength on the equilibrium sorption capacity of ampicillin by ACAF (time = 60 min, C_0 = 25 mg/L, pH = 7, ACAF mass = 0.8 g/L, and temperature = 25 °C)

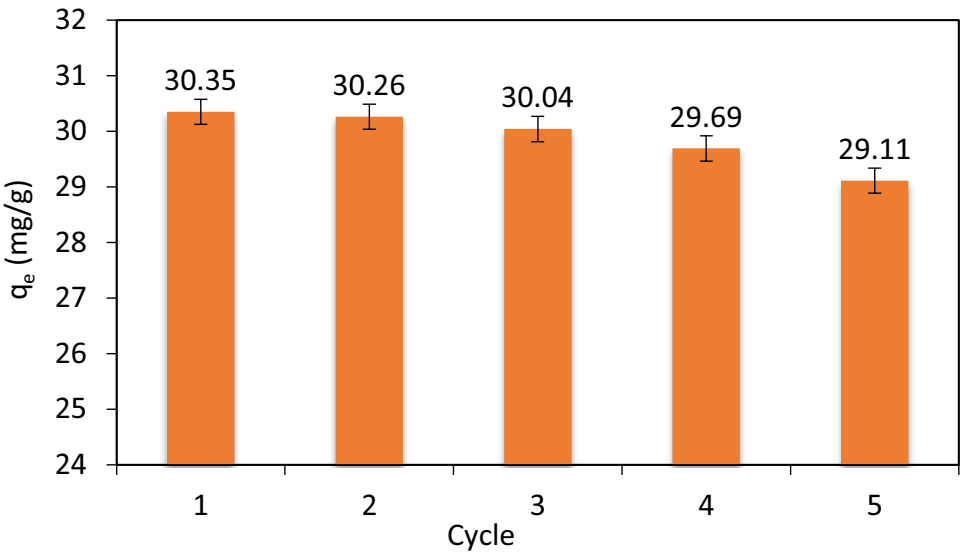

Fig. 10 Effect of regeneration on the equilibrium sorption capacity of ampicillin by ACAF (time = 60 min, C_0 = 25 mg/L, pH = 7, ACAF mass = 0.8 g/L, temperature = 25 °C)

ampicillin adsorption. On the basis of this, a lack of competition between added ions and ampicillin for adsorption and a lack of influence of electrostatic shielding effect on adsorption capacity sites can be concluded [55].

3.8 Reusability of ACAF

Regeneration studies which are conducted for examining the reusability of adsorbents are essential to comprehend whether the studied adsorbent is suitable for practical applications [56]; to understand the mentioned factor for adsorbent used in this study, and the adsorption–desorption process of ampicillin was considered for five cycles (Fig. 10). According to the figure, in each cycle, compared to the former cycle, a decrease in the adsorption capacity of ACAF could be detected. In cycle no. 1, the adsorption capacity of ACAF for 25 mg/L ampicillin was observed to be 30.35 mg/g (%97.12), while it reached 29.11 mg/g (93.17) in cycle no. 5. This low decrease is representative of the potential regeneration and reusability of ACAF in the adsorption treatment systems.

4 Conclusion

According to the results of the present study, the BET surface area of chemically activated ACAF was high and equal to 716.4 m^2/g. The SEM analysis employed was indicative of the rough and porous surface of the synthesized adsorbent; it confirms the good properties of the adsorbent properties and potential for employment in the adsorption processes. Additionally, using the Langmuir, Freundlich, Temkin, and D-R isotherm models, the experimental data were analyzed, and the better applicability of the Langmuir isotherm for describing the data was ratified. Moreover, based on correlation coefficients values (R^2) obtained for kinetic models, PSO was more effective in explaining the data. Optimum values of the contact time and pH for offering highest adsorption efficiency were 60 and 7 min, respectively. The highest adsorption capacity of the studied adsorbent was identified to be about 114.3 mg/g (45 °C). This is representative of a high potential of it for ampicillin removal. Furthermore, the spontaneous and endothermic nature of ampicillin adsorption onto ACAF was proven based on thermodynamic studies. The above-mentioned results present ACAF as a promising adsorbent for removing residual ampicillin from polluted water.

Supplementary Information The online version contains supplementary material available at https://doi.org/10.1007/s13399-021-01962-4.

Acknowledgements The researchers would like to thank Zahedan University of Medical Sciences (Iran) for financial support and assistance in performing the experiments outlined in this study (code:10478)

References

1. Chen WR, Huang CH (2010) Adsorption and transformation of tetracycline antibiotics with aluminum oxide. Chemosphere 79:779–785
2. Adrianoa WS, Veredasb V, Santanab CC, Gonçalves LRB (2005) Adsorption of amoxicillin on chitosan beads: kinetics, equilibrium and validation of finite bath models. Biochem Eng J 27(2):132–137
3. Vecchio PD, Haro NK, Souza FS, Marcilio NR, Feris LS (2019) Ampicillin removal by adsorption onto activated carbon: kinetics, equilibrium and thermodynamics. Water Sci Technol 79(10):2013–2021
4. Anggraini M, Kurniawan A, Ong LK, Martin MA, Liu JC (2014) Antibiotic detoxification from synthetic and real effluents

using a novel MTAB surfactant-montmorillonite sorbent. RSC Adv 4:16298–16311
5. Nairi V, Medda L, Monduzzi M, Salis A (2017) Adsorption and release of ampicillin antibiotic from ordered mesoporous silica. J Colloid Interface Sci 497:217–225
6. Doroudi Z, Sarvestani MR (2020) Boron nitride nanocone as an adsorbent and senor for Ampicillin: a computational study. Chem Rev Lett 3:110–116
7. Kümmerer K (2009) Antibiotics in the aquatic environment – a review – Part I. Chemosphere 75(4):417–434
8. Erşan M, Bağd E (2013) Investigation of kinetic and thermodynamic characteristics of removal of tetracycline with sponge like, tannin based cryogels. Colloids Surf B. 104:75–82
9. Peng H, Pana B, Wu M, Ran Liu R, Zhanga D, Wu D, Xing B (2012) Adsorption of ofloxacin on carbon nanotubes: solubility, pH and cosolvent effects. J Hazard Mater 211–212:342–348
10. Balarak D, Mahdavi Y, Bazrafshan E, Mahvi AH (2016) Kinetic, isotherms and thermodynamic modeling for adsorption of acid blue 92 from aqueous solution by modified azolla filicoloides. Fres Environ Bullet 25(5):1321–1330
11. Khodadadi M, Panahi AH, Al-Musawi T, Ehrampoush MH, Mahvi AH (2019) The catalytic activity of $FeNi_3$@SiO_2 magnetic nanoparticles for the degradation of tetracycline in the heterogeneous Fenton-like treatment method. J Water Process Eng 32: 100943
12. Balarak D, Azarpira H (2016) Rice husk as a biosorbent for antibiotic metronidazole removal: isotherm studies and model validation. Int J ChemTech Res 9(7):566–573
13. Choi KJ, Kim SG, Kim SH (2008) Removal of antibiotics by coagulation and granular activated carbon filtration. J Hazard Mater 151:38–43
14. Melillo M, Gun'ko VM, Tennison SR, Mikhalovska LI, Phillips GJ, Davies JG (2004) Structural characteristics of activated carbons and ibuprofen adsorption affected by Bovine serum albumin. Langmuir 20:2837–2851
15. Garoma T, Umamaheshwar SH, Mumper A (2010) Removal of sulfadiazine, sulfamethizole, sulfamethoxazole, and sulfathiazole from aqueous solution by ozonation. Chemosphere 79:814–820
16. Balarak D, Mostafapour FK (2019) Photocatalytic degradation of amoxicillin using UV/Synthesized NiO from pharmaceutical wastewater. Indones J Chem 19:211–218
17. Mestre AS, Pires J, Nogueira JMF, Carvalho AP (2007) Activated carbons for the adsorption of ibuprofen. Carbon 45:1979–1988
18. Mestre AS, Pires J, Nogueira JMF, Parra JB (2007) Waste-derived activated carbons for removal of ibuprofen from solution: role of surface chemistry and pore structure. Bioresour Technol 100:1720–1726
19. Rostamian R, Behnejad H (2016) A comparative adsorption study of sulfamethoxazole onto graphene and graphene oxide nanosheets through equilibrium, kinetic and thermodynamic modeling. Proc Saf Environ Prot 102:20–29
20. Huang L, Wang M, Shi C, Huang J, Zhang B (2014) Adsorption of tetracycline and ciprofloxacin on activated carbon prepared from lignin with H_3PO_4 activation. Desalin Water Treat 52:2678–2687
21. Zhu XD, Wang YJ, Sun RJ, Zhou DM (2013) Photocatalytic degradation of tetracycline in aqueous solution by nanosized TiO_2. Chemosphere 92:925–932
22. Parolo ME, Savini MC, Vallés JM, Baschini MT, Avena MJ (2008) Tetracycline adsorption on montmorillonite: pH and ionic strength effects. Appl Clay Sci 40:179–186
23. Ji L, Chen W, Duan L, Zhu D (2009) Mechanisms for strong adsorption of tetracycline to carbon nanotubes: a comparative study using activated carbon and graphite as adsorbents. Environ Sci Technol 43:2322–2327
24. Zhang L, Song X, Liu X, Yang L, Pan F (2011) Studies on the removal of tetracycline by multi-walled carbon nanotubes. Chem Eng J 178:26–33
25. Carabineiro A, Thavorn-Amornsri T, Pereira F, Figueiredo L (2011) Adsorption of ciprofloxacin on surface modified carbon materials. Water Res 145:4583–4591
26. Balarak D, Baniasadi M, Lee SM, Shim MJ (2021) Ciprofloxacin adsorption onto azolla filiculoides activated carbon from aqueous solutions. Desalin Water Treat 218:444–453
27. Dyanati RA, Yousefi ZA, Cherati JY, Belarak D (2013) Investigating phenol absorption from aqueous solution by dried azolla. J Mazand Uni Med Sci 22(2):13–20
28. Balarak D, Al-Musawi T, Mohammed IA, Abasizadeh H (2020) The eradication of reactive black 5 dye liquid wastes using Azolla fliculoides aquatic fern as a good and an economical biosorption agent. SN Appl Sci 2: 1015
29. Mahvi AH, Mostafapour FK (2018) Biosorption of tetracycline from aqueous solution by azolla filiculoides: equilibrium kinetic and thermodynamics studies. Fres Environ Bullet 27:5759–5767
30. Dyanati-Tilaki RA, Yousefi Z, Yazdani-Cherati J (2013) The ability of azolla and lemna minor biomass for adsorption of phenol from aqueous solutions. J Mazand Uni Med Sci 23(106):140–146
31. Balarak D, Azarpira H, Mostafapour FK (2016) Study of the adsorption mechanisms of cephalexin on to Azolla filiculoides. Pharm Chem 8:114–121
32. Peng X, Hu F, Dai H, Xiong Q (2016) Study of the adsorption mechanism of ciprofloxacin antibiotics onto graphitic ordered mesoporous carbons. J Taiwan Inst Chem Eng 8:1–10
33. Nasseh N, Khosravi R, AbuRumman G, Ghadirian M, Eslamid H, Khoshnamvand M, Al-Musawi T, Khosravi A (2021) Adsorption of Cr(VI) ions onto powdered activated carbon synthesized from *Peganum harmala* seeds by ultrasonic waves activation. Environ Technol Innovation 101277
34. Jafari M, Aghamiri SF, Khaghanic G (2011) Batch adsorption of cephalosporins antibiotics from aqueous solution by means of multi-walled carbon nanotubes. World Appl Sci J 14:1642–1650
35. Wu Y, Liu W, Wang Y, Hu X, He Z, Chen X (2018) Enhanced removal of antibiotic in wastewater using liquid nitrogen-treated carbon material: material properties and removal mechanisms. Int J Environ Res Public Health 15(12):2652
36. Rahardjo AK, Susanto MJJ, Kurniawan A, Indraswati N, Ismadji S (2011) Modified Ponorogo bentonite for the removal of ampicillin from wastewater. J Hazard Mater 190:1001–1008
37. Queiroz AC, Santos JD, Monteiro FJ (2005) Adsorption isotherm of sodium ampicillin onto dense and porous hydroxyapatite. Key Eng Mater 284–286:387–390
38. Rahman N, Varshney P (2020) Assessment of ampicillin removal efficiency from aqueous solution by polydopamine/zirconium(IV) iodate: optimization by response surface methodology. RSC Adv 10:20322–20337
39. Chitongo R, Opeolu BO, Olatunji OS (2019) Abatement of amoxicillin, ampicillin, and chloramphenicol from aqueous solutions using activated carbon prepared from grape slurry. Clean: Soil Air Water 47:1800077
40. Yang H, Liu Q (2015) Hierarchically-organized, well-dispersed hydroxyapatite-coated magnetic carbon with combined organics and inorganics removal properties. Chem Eng J 275:152–159
41. Balarak D, Mostafapour FK, Azarpira H (2016) Adsorption isotherm studies of tetracycline antibiotics from aqueous solutions by maize stalks as a cheap biosorbent. Int J Pharm Technol 8:16664–16675
42. Balarak D, Mostafapour FK, Bazrafshan E, Saleh TA (2017) Studies on the adsorption of amoxicillin on multi-wall carbon nanotubes. Water Sci Technol 75:1599–1606

43. Behera SK, Oh SY, Park HS (2012) Sorptive removal of ibuprofen from water using selected soil minerals and activated carbon. Int J Environ Sci Technol 9:85–94
44. Heckmann LH, Helen AC, Hooper L, Connon R, Hutchinson TH, Maund SJ, Sibly RM (2007) Chronic toxicity of ibuprofen to Daphnia magna: effects on life history traits and population dynamics. Toxicol Lett 172:137–145
45. Al-Khalisy R, Al-Haidary A, Al-Dujaili A (2010) Aqueous phase adsorption of cephalexin onto Bebntonite and activated carbon. Sep Sci Technol 45:1286–1294
46. Ghauch A, Tuqan A, Assi HA (2009) Elimination of amoxicillin and ampicillin by micro scale and nano scale iron particles. Environ Pollut 157:1626–1635
47. Ahmadi S, Banach A, Mostafapour FK (2017) survey of cupric oxide nanoparticles in removal efficiency of ciprofloxacin antibiotic from aqueous solution: adsorption isotherm study. Desalin Water Treat 89:297–303
48. Balarak D, Taheri Z, Shim MJ, Lee SM, Jeon C (2021) Adsorption kinetics and thermodynamics and equilibrium of ibuprofen from aqueous solutions by activated carbon prepared from lemna minor. Desalin Water Treat 215:183–193
49. Chih-Jen W, Zhaohui L, Wei-The J (2011) Adsorption of ciprofloxacin on 2:1 dioctahedral clay minerals. Appl Clay Sci 53:723–728
50. Fakhri A, Rashidi S, Asif M, Tyagi I, Agarwal S, Gupta VK (2016) Dynamic adsorption behavior and mechanism of Cefotaxime, Cefradine and Cefazolin antibiotics on CdS-MWCNT nanocomposites. J Mol Liq 215:269–275
51. Liu H, Liu W, Zhang J, Zhang C, Ren L, Li Y (2011) Removal of cephalexin from aqueous solution by original and Cu(II)/Fe(III) impregnated activated carbons developed from lotus stalks kinetics and equilibrium studies. J Hazard Mater 185:1528–1535
52. Bazrafshan E, Sobhanikia M, Mostafapour FK (2017) Chromium biosorption from aqueous environments by mucilaginous seeds of Cydonia oblonga: kinetic and thermodynamic studies. Global Nest J 19(2):269–277
53. Peterson JW, Petrasky LJ, Seymourc MD (2012) Adsorption and breakdown of penicillin antibiotic in the presence of titanium oxide nanoparticles in water. Chemosphere 87:911–917
54. Yu F, Li Y, Han S, Jie M (2016) Adsorptive removal of antibiotics from aqueous solution using carbon Materials. Chemosphere 153:365–385
55. Baccar R, Sarrà M, Bouzid J, Feki M, Blánquez P (2012) Removal of pharmaceutical com-pounds by activated carbon prepared from agricultural by-product. Chem Eng J 211:310–317
56. Balarak D, Mahvi AH, Shim MJ, Lee SM (2021) Adsorption of ciprofloxacin from aqueous solution onto synthesized NiO: isotherm, kinetic and thermodynamic studies. Desalin Water Treat 212:390–400